NASA TECHNICAL MEMORANDUM

NASA TM X-52924

NASA TM X-52924

RE-EXAMINATION OF HEAT PIPE STARTUP

by Peter M. Sockol and Ralph Forman
Lewis Research Center
Cleveland, Ohio

TECHNICAL PAPER proposed for presentation at
1970 Thermionic Conversion Specialist Conference sponsored
by the Institute of Electrical and Electronics Engineers
Miami, Florida, October 26-29, 1970

RE-EXAMINATION OF HEAT PIPE STARTUP

Peter M. Sockol and Ralph Forman
NASA-Lewis Research Center
Cleveland, Ohio 44135

Abstract

In a lithium heat pipe high operating temperatures permit visual observation of the temperature profile during startup. Cotter's model of the startup process is reassessed in the light of these observations. The model is modified by moving the sonic point to the end of the hot zone and including the opposing effects of wall friction and condensation on the flow. Transient measurements have been made on a lithium heat pipe for startup to temperatures in the range 1000 to 1400° C. As predicted by the theory, the temperature of the hot zone is fairly independent of the power input to the evaporator until the hot zone reaches the end of the pipe. The hot zone temperature predicted by the theory is 50 to 80° C higher than the measured value with up to 30° C of the discrepancy attributable to the measurement.

Introduction

Most of the interest in heat pipe startup is limited to the conditions under which a pipe can or cannot be started. Nevertheless, when the heat pipe is part of a structure designed to operate at a high temperature and composed of materials with different coefficients of expansion, it may be necessary to have detailed information about the performance of the pipe during startup. In the case of a heat-pipe-cooled fast reactor, where the reactivity is dependent on the temperature of the materials, the performance of the heat pipes during startup is especially important.

In a lithium heat pipe high operating temperatures permit visual observation of the temperature profile during startup. At sufficiently high heat inputs the temperature is seen to rise to some intermediate level and remain almost constant as a steep temperature front moves down the pipe. When the uniform hot zone fills the pipe, the temperature increases to its steady state value. In Cotter's model of the startup process[1] it is assumed that the vapor flow is sonic at the end of the evaporator. This, however, would require a substantial temperature drop at this point[2] which is not observed. It is more logical to assume a sonic point at the end of the hot zone near the sharp temperature front.

In the present work a modified version of Cotter's analysis is applied to the startup of a radiation-cooled heat pipe. Particular attention is focused on the vapor flow in the evaporating and condensing sections of the hot zone. To check the analysis transient measurements were made on a lithium heat pipe during startup to temperatures of 1000 to 1400°C. Temperature vs time histories were recorded at equally spaced points on the condensor. Numerical calculations of the temperature and length of the hot zone vs time are compared with the experimental values.

Theory

Following Cotter,[1] it is assumed that the wall temperature T in the hot zone is uniform and the cold zone remains at the initial temperature T_i. The state of the heat pipe at time t is pictured in figure 1. Here ℓ_e is the evaporator length, ℓ is the length of the hot portion of the condensor, Q is the heat input to the evaporator, and q is the radiation per unit length from the hot zone.

Energy balances on the evaporator and condensor give

$$C\ell_e \frac{d}{dt}(T-T_i) = Q - q\ell_e - w_e h_{fg}, \quad (1)$$

$$C\frac{d}{dt}\ell(T-T_i) = w_e h_{fg} - q\ell, \quad (2)$$

where w_e is the mass flow rate of vapor leaving the evaporator, h_{fg} the heat of vaporization, and C the heat capacity per unit length of the wall, liquid and wick. The heat capacity of the vapor is negligible, despite the large heat of vaporization, because the vapor density is very small. In addition the heat of fusion is neglected even though this produces a noticeable effect for values of T_i below the melting point.

When the hot zone fills the pipe and $\ell = \ell_c$, Eqs. (1) and (2) give

$$C(\ell_e+\ell_c)\frac{d}{dt}(T-T_i) = Q - q(\ell_e+\ell_c). \quad (3)$$

This describes the final approach to the steady state.

In evaluating the flow rate w_e it is assumed that the vapor velocity becomes sonic at the end of the hot zone. In the condensing portion of the hot zone wall friction increases the Mach number and condensation decreases it.[3] Hence, the above assumption requires that the effects of wall friction predominate. This is probable if most of the condensation occurs just down stream of the sonic point where the wall is cold. As T is approximately constant while the temperature front moves down the pipe, the condensation rate per unit length m is given by q/h_{fg}. From Eq. (1) with T constant $w_e h_{fg} = Q - q\ell_e$. Thus, the present model imposes the requirement that $Q >> q(\ell_e+\ell)$ for $\ell < \ell_c$; this is true when the steady state temperature is well above the intermediate value of T during the motion of the front. In addition it is assumed that the difference between the stagnation temperature of the flowing vapor and the temperature of the evaporating or condensing vapor is everywhere small relative to the vapor temperature and that heat conduction to or from the vapor is negligible. Under these conditions the stagnation temperature is approximately constant. Finally, since the velocity of the front is small relative to the vapor velocities, it is assumed that steady flow equations are applicable.

Upstream of the sonic point the equation for the Mach number M, in the one-dimensional approximation, is written[3]

$$\frac{dM^2}{M^2} = \frac{1+\frac{1}{2}(k-1)M^2}{1-M^2}\left[kM^2\frac{d\lambda}{D} - 2(1+kM^2)\frac{m\,d\lambda}{w}\right], \quad (4)$$

Prepared for the 1970 Thermionic Conversion Specialists Conference, October 26 through 29, 1970 Miami, Florida.

where k is the ratio of specific heats, f the friction factor, D the passage diameter, w the mass flow rate, and x the axial coordinate. If the flow is laminar and the wall Reynolds number $m/2\pi\mu$, where μ is the viscosity, is of order one or less, the velocity profile is essentially parabolic[4] and f is given by

$$f \approx 64/R_x = 16\pi\mu D/w, \qquad (5)$$

where R_x is the axial Reynolds number. For constant m, $w = w_e - mx$. Elimination of f and w from Eq. 4 gives

$$\frac{dM^2}{M^2} = \frac{1+\frac{1}{2}(k-1)M^2}{1-M^2}\,2(bM^2-1)\,\frac{m\,dx}{w_e - mx}, \qquad (6)$$

with $b = k(8\pi\mu/m-1)$. From Eq. (6) it is seen that it is necessary to have $bM^2 > 1$ at the end of the evaporator if M is to increase in the condensor. Integration of Eq. (6) from x = 0 to ℓ, where M = 1, gives

$$-2\ln\left(1-\frac{m\ell}{w_e}\right) = \ln(1-N) - [b+\tfrac{1}{2}(k-1)]^{-1} \cdot \left[(b-1)\ln\left(1-\frac{b}{b-1}N\right) + \tfrac{1}{2}(k+1)\ln\left(1-\frac{k-1}{k+1}N\right)\right], \qquad (7)$$

with $N = 1 - M_e^2$.

In the evaporator it is assumed that the effects of wall friction are negligible compared to those of evaporation. The one-dimensional flow equations can be integrated to give[3]

$$\frac{w}{w^*} = \frac{M[2(k+1)]^{\frac{1}{2}}}{1+kM^2}\left[1+\tfrac{1}{2}(k-1)M^2\right]^{\frac{1}{2}}, \qquad (8)$$

where w^* is the value of w at M = 1. From the definitions of w and M, $w/M = \rho a A$ where ρ and a are the density and speed of sound of the vapor and A is the cross-section of the passage. Thus, Eq. (8) at M = 0 gives

$$w^* = \rho_o a_o A\,[2(k+1)]^{-\frac{1}{2}}, \qquad (9)$$

where ρ_o and a_o are values at the beginning of the evaporator. At the end of the evaporator, where $M^2 = M_e^2 = 1 - N$, Eq. (8) gives

$$w_e = w^*(1-N)^{\frac{1}{2}}\left(1-\frac{k-1}{k+1}N\right)^{\frac{1}{2}}\left(1-\frac{k}{k+1}N\right)^{-1}. \qquad (10)$$

Note that $\rho_o a_o = p_o\sqrt{k/RT}$ where p_o is the vapor pressure at temperature T and R is the gas constant per unit mass of vapor. Thus w^* is a very strong function of T.

Equations (1) and (2) are integrated numerically to obtain T and ℓ as functions of t. At each point in time Eqs. (7) and (10) must be solved simultaneously to obtain N and w_e.

Experiment

A 14 in. long, 0.5 in. diameter lithium filled heat pipe has been designed and fabricated for experiments on startup characteristics. The containment envelope for the pipe is T-111, an alloy of 90% Ta, 8% W, and 2% Hf. The wick structure is a composite made of Ta screen (150 mesh and 0.002 in. diam. wire) and fabricated as an 0.008 in. thick porous tube by swaging techniques. The wick is employed in a concentric annulus design as described in ref. 5. The annular gap is 0.017 in.

A sketch of the experimental apparatus is shown in figure 2. The heat pipe is supported in a quartz tube by lucalox spacers, and the evaporator is heated over 5 in. of its length by induction heating. Three thermocouples (W, 5%-Re; W, 26%-Re) are spaced 0.5 in. apart on the condensor end of the pipe. The quartz tube is evacuated by a turbomolecular pump and the thermocouple leads are taken out through a side arm connected to the quartz tube. Black body holes are machined in the evaporator and condensor end caps. These are used to obtain independent temperature measurements and estimates of the spectral emissivity of the heat pipe surface.

Experimental data on the startup characteristics are obtained as follows. With the quartz tube evacuated to the range of 2×10^{-7} torr, the induction heater is switched on to a constant power level (e.g. 1 kw). As the temperature of the pipe increases, the thermocouple readings at positions 1 to 3 (fig. 2) are recorded on a four-pen strip chart recorder. These readings are complemented by visual observation of the temperature profile along the pipe as a function of time. The temperature of the evaporator is observed to rise to the range of 800 to 900° C and then remain relatively constant as a temperature front moves down the pipe. In approximately one minute the whole pipe reaches this intermediate temperature and then behaves isothermally as the temperature increases to a steady state value determined by a balance between the heat input and the radiation losses. When a steady state is reached, the recorder measurements are checked with a standard potentiometer. A comparison between thermocouple and optical pyrometer readings (corrected for emissivity) shows a deviation of up to 30° C with the pyrometer readings consistently higher.

Figure 3 shows some typical data obtained at a heat input in the range of 1 kw. as the temperature front moved by the thermocouple positions. The origin of the time scale is arbitrary. The curves go through a small bump corresponding to the melting of lithium at 180° C and then remain fairly parallel as they rise to the intermediate temperature of 850° C. The final increase of the joined curves is quite marked and corresponds to the assymptotic approach to the steady state temperature of 1235° C.

From the spacing of the curves, in both distance and time, the velocity $\dot{x}$ of the temperature front is estimated as 1.1 cm/s. Since the curves are parallel to each other, it can be inferred that the shape of the front is constant and that a point moving with the front remains at the same temperature. Hence, at a fixed point x on the surface of the pipe, $\partial T/\partial t + \dot{x}\,\partial T/\partial x = 0$, and the curves of figure 3 can be used to construct the temperature profile of the front. In particular the maximum temperature gradient of the front is 260° C/cm which indicates the steepness of the front.

Comparison of Theory and Experiment

Figure 4 shows the theoretical values of the temperature T and length ($\ell_e + \ell$) of the hot zone for the case represented by the data of figure 3. As the heat input from the induction heater is not known, the measured steady state temperature (1235° C) and an assumed total emissivity of 0.3 were used to obtain an approximate value of 1.25 kw. for Q. The intermediate temperature of 905° C obtained from the theory exceeds the experimental value by 55° C. As much as 30° C of this difference may, however, be due to errors in the thermocouple readings. The remaining 25° C is quite acceptable when the approximate nature of the theory is considered. From the plot of ($\ell_e + \ell$) vs time a mean velocity of 0.95 cm/s is obtained for the front. This compares favorably with the value of 1.1 cm/s estimated from the data. Finally, the theoretical values of the intermediate temperature are compared

with the measured values for three other cases in the following table.

Steady state temp.	(°C)	1080	1190	1290
Calc. heat input	(kw.)	0.80	1.10	1.43
Intermediate temp.				
theory	(°C)	875	895	915
experiment	(°C)	810	830	840

Note that, while the intermediate temperature predicted by the theory is consistently high, the weak variation of this temperature with heat input obtained from the theory is in close agreement with experiment.

Concluding Remarks

On the basis of the satisfactory agreement between theory and experiment obtained in the present work we conclude that the theory provides an adequate description of the heat pipe startup process. In addition from analysis of temperature profiles extracted from data similar to that of figure 3, it is hoped that the local condensation rate down stream of the temperature front can be obtained. This information is needed before the present theory can be used for heat transfer calculations during the startup of a complex structure like a heat-pipe-cooled, fast reactor.

STATE OF HEAT PIPE AT TIME t

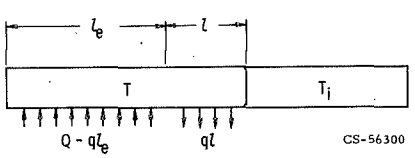

Fig. 1

EXPERIMENTAL APPARATUS

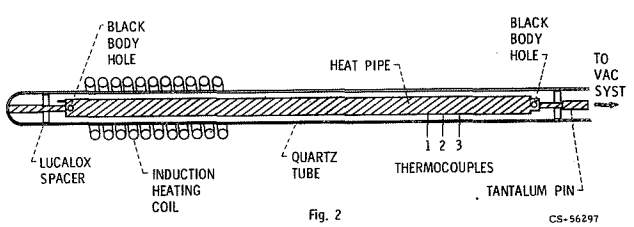

Fig. 2

References

1. T. P. Cotter, IEEE Therm. Conv. Spec. Conf., Palo Alto (1967), p. 344.
2. J. E. Kemme, IEEE Therm. Conv. Spec. Conf., Framingham (1968), p. 266.
3. A. H. Shapiro, "The Dynamics and Thermodynamics of Compressible Fluid Flow," Rondald Press, New York, 1953, Vol. I, Ch. 8.
4. F. M. White, Jr., B. F. Barfield, and M. J. Goglia, J. Appl. Mech. 25, 613 (1958).
5. Los Alamos Scientific Laboratory, quarterly status report LA-4109-MS, Feb. 1969.

MEASURED TEMPERATURE VS TIME AT CONDENSER

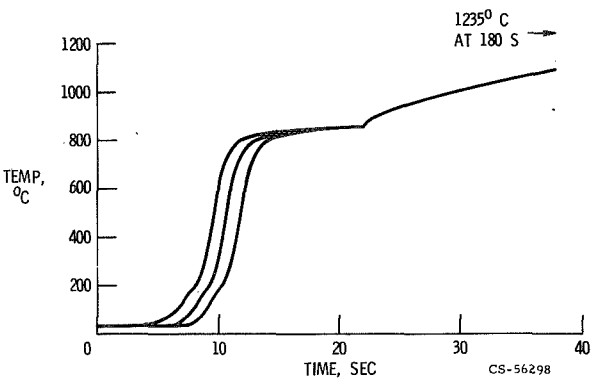

Fig. 3

CALCULATED TEMPERATURE AND LENGTH OF HOT ZONE VS TIME

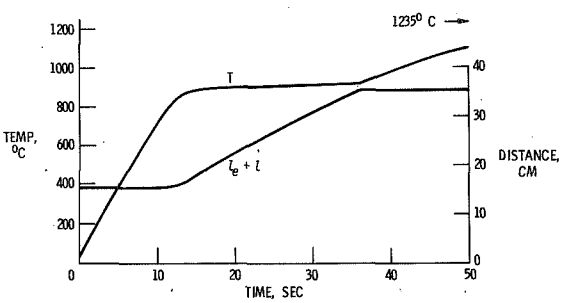

Fig. 4

NASA-Lewis